

Table of Contents

Cover pages and budget summary	
Table of contents	1
Scientific/technical/management section (15 pages)	
1 – “A comprehensive picture of the Mars upper atmosphere and ionosphere”	2
2 – Testing dayside ionospheric predictions in the topside and at the main peak	5
3 – Task A: Topside structure	7
4 – Task B: Topside composition	8
5 – Task C: Electron density at the main peak	9
6 – Task D: The neutral pressure at the main peak	11
7 – Task E: Support for spacecraft operations inside the atmosphere	12
8 – The Boston University Mars Ionospheric Model	13
9 – Relevance to NASA and the MAVEN Participating Scientist Program	14
10 – Personnel and Work Plan	15
References	16
Biographical Sketch for PI Paul Withers	23
Current and Pending Support for PI Paul Withers	25
Budget Narrative	27

1 – “A comprehensive picture of the Mars upper atmosphere and ionosphere”

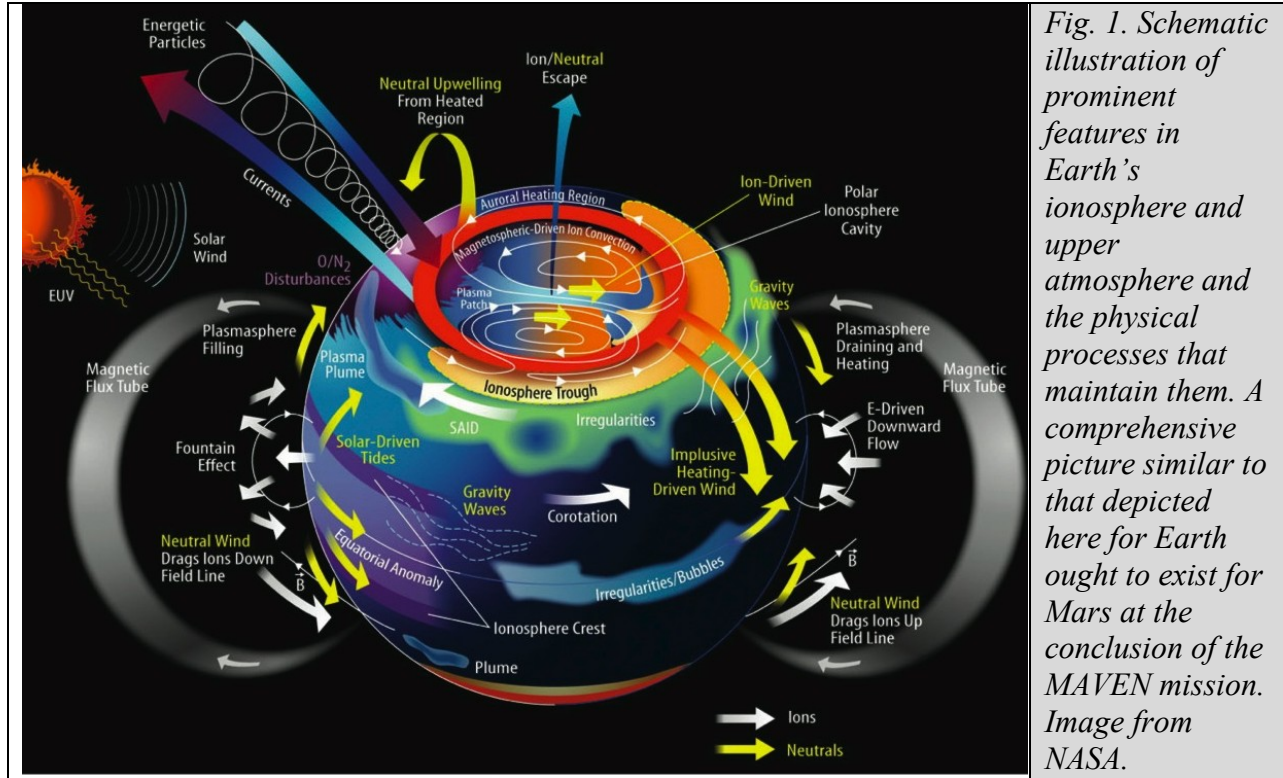


Fig. 1. Schematic illustration of prominent features in Earth's ionosphere and upper atmosphere and the physical processes that maintain them. A comprehensive picture similar to that depicted here for Earth ought to exist for Mars at the conclusion of the MAVEN mission. Image from NASA.

The MAVEN Concept Study Report opens by saying “The MAVEN mission will provide a comprehensive picture of the Mars upper atmosphere, ionosphere, solar energetic drivers, and atmospheric losses. It will deliver definitive answers to long-standing questions about the climate history and habitability of Mars.” Figure 1, a comprehensive picture for Earth, illustrates the tremendous scope of MAVEN’s task.

In order to provide these definitive answers and satisfy Level 1 mission requirements, the MAVEN team must determine the state of the atmosphere and accompanying escape processes over the past 4.5 billion years. The MAVEN team must develop the best possible picture of current conditions and processes, then carefully extrapolate backwards in time. If the results of this long, long extrapolation are to be realistic, then understanding of current conditions and processes must be far better than it is today. This is reflected in MAVEN Science Question #1: What is the current state of the upper atmosphere and ionosphere, and what processes control it?

It might be thought that current understanding of the state of the upper atmosphere and ionosphere is quite advanced. After all, many complex numerical models are used today to simulate aspects of the upper atmosphere, ionosphere, magnetosphere, and space environment (e.g., Angelats i Coll et al., 2004, 2005; Bell et al., 2007; Bougher et al., 2002, 2006, 2008; Brain et al., 2010; Brecht and Ledvina, 2006; Fang et al., 2010a, b; Forget et al., 1999; Fox, 2004, 2009; Fox and Yeager, 2006; Fox et al., 1996; Gonzalez-Galindo et al., 2005, 2009a, b, 2010; Krasnopolsky, 2002; Leblanc and Johnson, 2002; Liemohn et al., 2006; Lollo et al., 2012;

INTEGRATION OF MAVEN NEUTRAL AND PLASMA OBSERVATIONS

Mendillo et al., 2011; Ma et al., 2004; Ma and Nagy, 2007; McDunn et al., 2010; Modolo et al., 2006; Moffat-Griffin et al., 2007; Shinagawa and Cravens, 1989; Valeille et al., 2009a, b, 2010).

These models can make detailed predictions concerning almost anything scientists want to know about these regions of the Mars system. They stand ready to ingest anticipated MAVEN data, simulate 4.5 billion years of history, and report “the total loss to space through time” (MAVEN Science Question #3). The Science Closure presentation by Lillis at the pre-AGU MAVEN Community Workshop described how the MAVEN team plans to use such models: a general theme was the use of MAVEN data as inputs to existing models. (We refer to the models that are included in the planned Science Closure work as “front-line” models.) The presented pathways to Science Closure did not include improving the front-line models based on observations. That is, MAVEN’s strategy for answering its key science questions uses today’s models.

Yet consider the limited data on which today’s models of the upper atmosphere and ionosphere are founded – two neutral composition profiles (Nier and McElroy, 1977); sparse neutral temperature profiles from Viking landers, aerobraking orbiters, and UV observations (e.g. Stewart et al., 1972; Seiff and Kirk, 1977; Withers, 2006; McDunn et al., 2010); no direct measurements of neutral winds (Bougher et al., 2013); two ion composition profiles (Hanson et al., 1977); two ion/electron temperature profiles (Hanson and Mantas, 1988); and no direct data on plasma motion (Withers, 2009). Figures 2-4 show some of these sparse constraints.

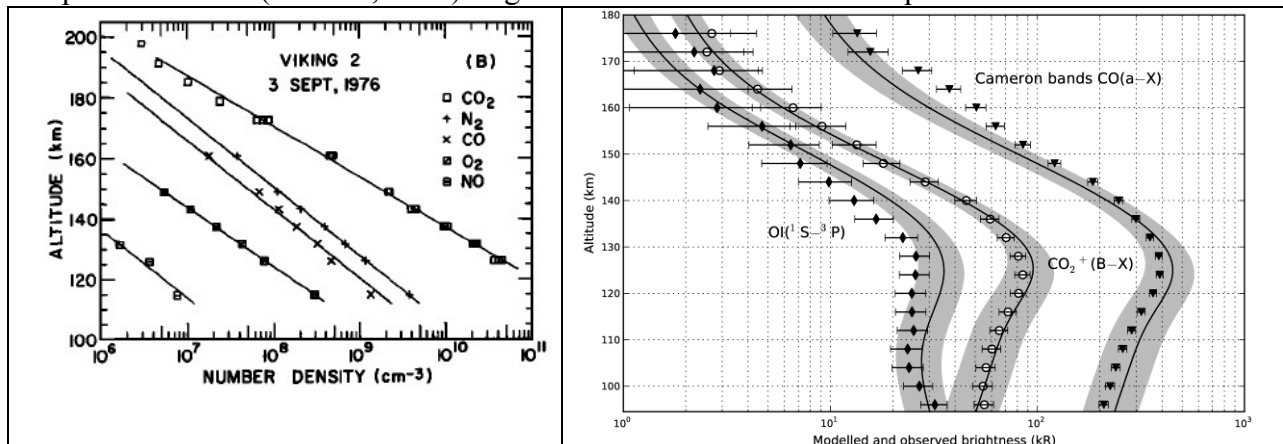


Fig. 2. Number densities of CO₂, N₂, CO, O₂, and NO as measured by Viking 2. This instrument was not sensitive to O, whose presence was inferred from ion composition data. From Figure 4 of Nier and McElroy (1977).

Fig. 3. SPICAM measurements (symbols) and predictions (shaded envelopes) for Cameron CO, CO₂⁺, and OI emissions. From Figure 14.12 of Bougher et al. (2013).

Even with today’s limited data, models fail to reproduce a range of observed features (Figure 5). The anticipated MAVEN datasets will only reveal more unexplained features. This demands model advancements. We postulate that MAVEN observations will lead to new discoveries about how the Mars system functions, which ought to be incorporated into the front-line models in order to achieve the best possible reconstruction of the history of the climate of Mars. MAVEN is going to revolutionize understanding of how the upper atmosphere and ionosphere of Mars function, and numerical models should be updated in response to these discoveries. There must be intermediate steps between the generation of calibrated data products and the application of complex large-scale models – analysis steps that integrate neutral, plasma, and other

INTEGRATION OF MAVEN NEUTRAL AND PLASMA OBSERVATIONS

observations to yield succinct statements about how the upper atmosphere and ionosphere behave. We propose to perform some of these critical steps, activities which are not included in the plans of the MAVEN team (as described in the Concept Study Report and pre-AGU Community Workshop).

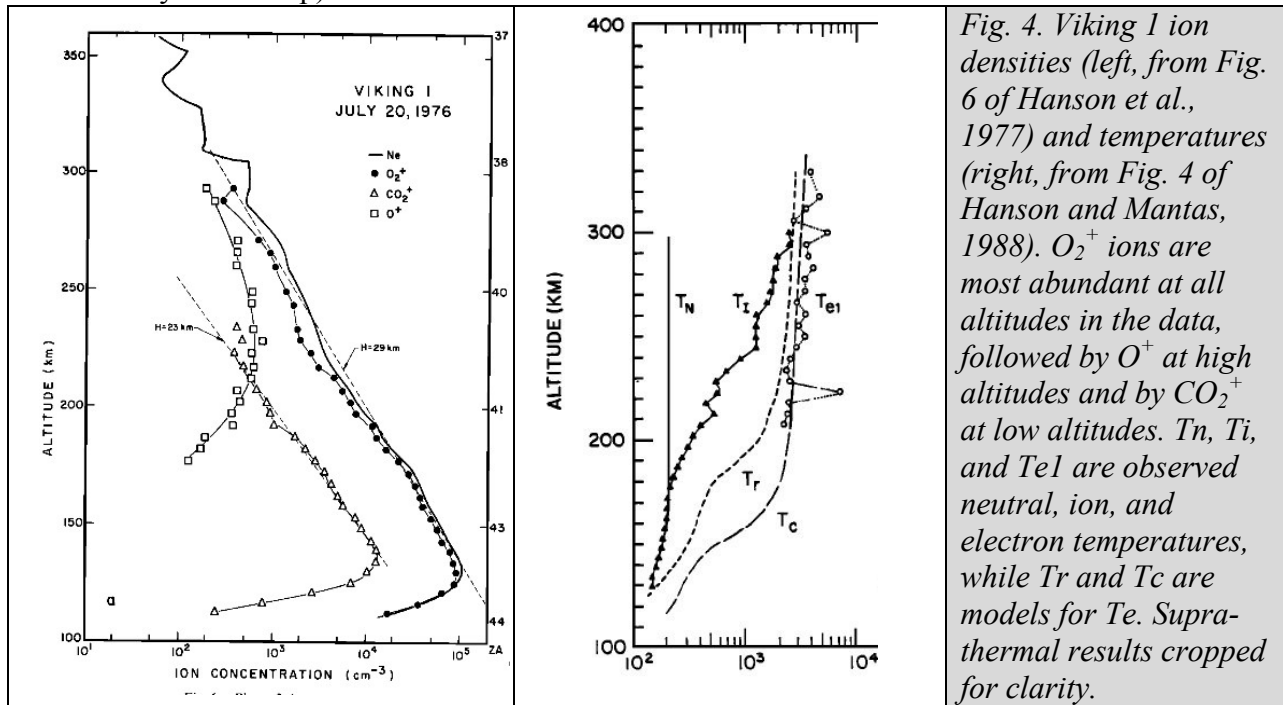


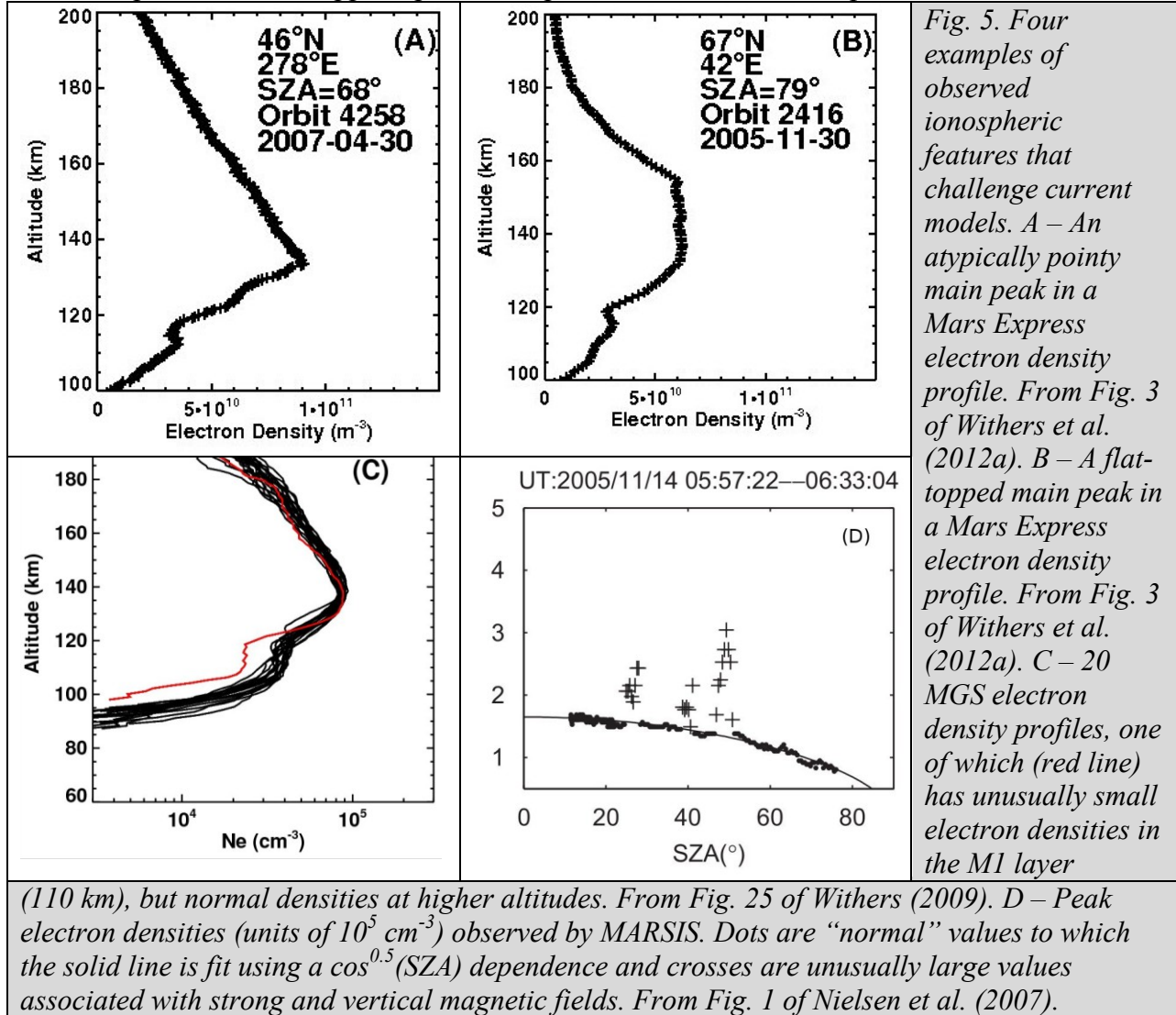
Fig. 4. Viking I ion densities (left, from Fig. 6 of Hanson et al., 1977) and temperatures (right, from Fig. 4 of Hanson and Mantas, 1988). O₂⁺ ions are most abundant at all altitudes in the data, followed by O⁺ at high altitudes and by CO₂⁺ at low altitudes. T_n, T_i, and T_e are observed neutral, ion, and electron temperatures, while T_r and T_c are models for T_e. Supra-thermal results cropped for clarity.

Our basic strategy is to analyze MAVEN data of the upper atmosphere and ionosphere, supported by a numerical model, in order to transform better knowledge of properties (the data) into better knowledge of processes (needed for extrapolation into the past). These findings can then be incorporated into the MAVEN front-line models in order to better reconstruct the climate history of Mars. Even if the front-line modelers elect not to improve their models during MAVEN's primary mission, our findings will still inform the work of the MAVEN team and contribute to building a comprehensive picture of the upper atmosphere and ionosphere (Fig. 1).

This approach requires experimentation using the chosen numerical model in order to uncover the underlying physical reasons behind a particular observed trend. As such, the numerical model must be easy to modify and not too resource-hungry. The established Boston University Mars Ionospheric Model is well-suited to this role, as outlined in Section 8. Many of the front-line, state-of-the-art models that are already available to MAVEN are complex and global-scale, taking considerable time to complete a single simulation, and hence are not suited to this role.

Our scientific goal, inspired by MAVEN Science Question #1, is to integrate MAVEN data from multiple instruments to determine how the state of the dayside ionosphere is influenced by the neutral atmosphere, solar flux, and magnetic environment. The primary way by which we shall address this goal is to test simple ionospheric predictions in the topside and at the main peak using MAVEN data, accompanied by interpretation with the Boston University Mars Ionospheric Model. This is a natural extension of our current research using existing datasets. Almost all necessary data are included in the MAVEN Key Parameter files that disseminate useable data around the MAVEN team rapidly and regularly (pre-AGU Community Workshop presentations).

Our work is divided into five Tasks, each of which also directly supports mission operations and decision-making. Task A examines the vertical structure of the topside ionosphere. Task B examines the composition of the topside ionosphere. Task C examines the peak electron density. Task D examines the neutral pressure at the ionospheric peak. Task E, which is strongly linked to mission operations, will support spacecraft operations inside the atmosphere.



2 – Testing dayside ionospheric predictions in the topside and at the main peak

The scientific literature contains many basic predictions concerning the ionosphere and neutral upper atmosphere of Mars, particularly as regards coupling between them (e.g., Barth et al., 1992; Withers, 2009; Bougher et al., 2013). Given MAVEN data, testing such theoretical predictions ought to be quite straightforward and will lead directly to the new insights about physical processes that are needed to reconstruct 4.5 billion years of climate evolution. The most valuable new insights will be found where these basic predictions fail. This concept motivates Tasks A-D, which will test the following predictions.

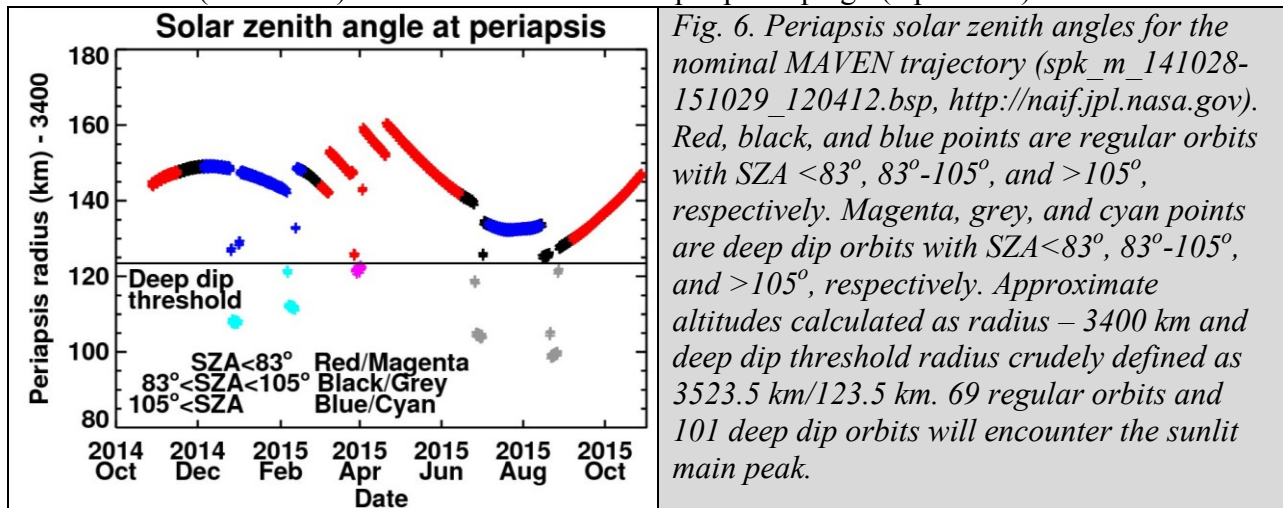
INTEGRATION OF MAVEN NEUTRAL AND PLASMA OBSERVATIONS

- **Task A:** The topside plasma scale height is thought to be related to either the neutral scale height (if plasma transport is suppressed by the magnetic field) or the plasma temperature (if plasma transport is not suppressed by the magnetic field) (Section 3).
- **Task B:** The composition of the topside ionosphere is thought to be an O^+/O_2^+ mixture, whereas the composition is dominated by O_2^+ at the main peak (Section 4).
- **Task C:** The peak electron density is thought to be a known function of solar flux, neutral scale height, and the electron temperature (Section 5).
- **Task D:** The peak altitude is thought to occur at a predictable pressure level (Section 6).

Are these predictions true? Are they always true? Does their validity depend on neutral composition, ionospheric temperature, or other properties of the ionosphere/upper atmosphere? Does their validity depend on local time, the magnetic environment, or other external influences? Our current research addresses such questions using pre-MAVEN data, providing a firm foundation for the proposed work.

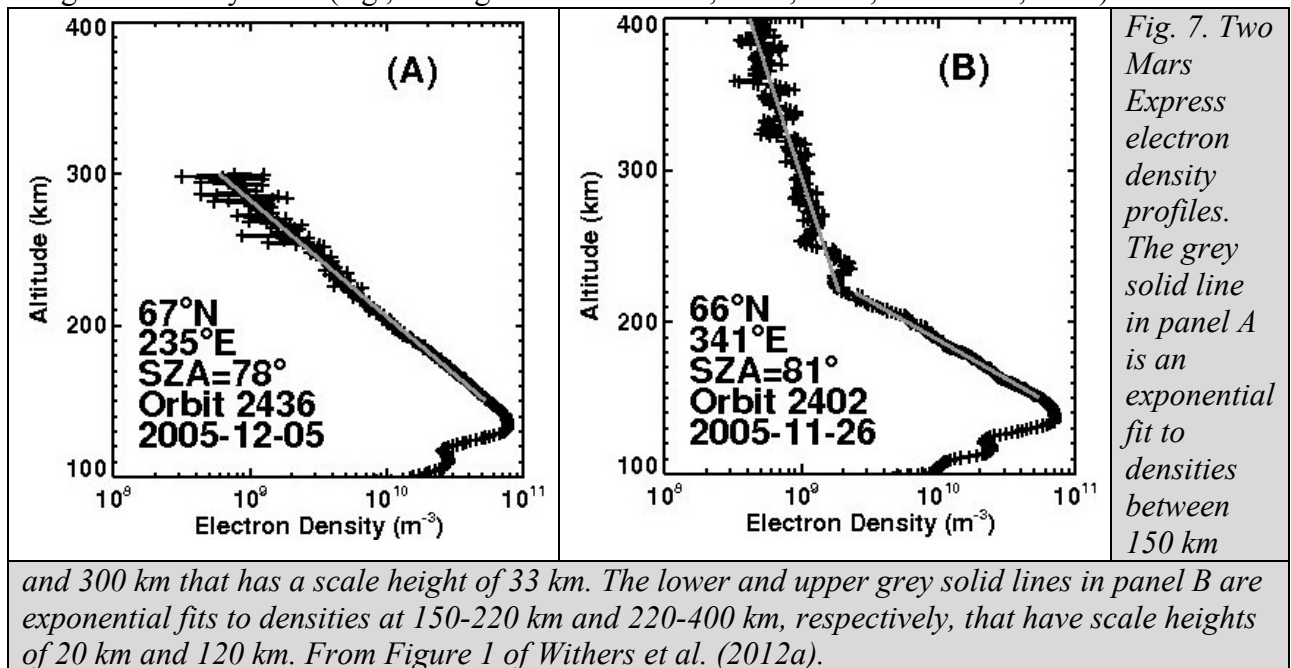
Ample dayside main peak data for Tasks C and D will be available from sunlit periapses. It is well-known that MAVEN will sample the main peak on five deep dip campaigns, yet it is less recognized that MAVEN will often encounter the main peak of the sunlit ionosphere on 150 km periapses. The peak height was above 150 km in 20% of MGS profiles at solar zenith angles (SZAs) of 83° - 90° and the sun does not set at ionospheric heights (120 km) until $SZA=105^\circ$ (Withers et al., 2012b). These main peak encounters at 150 km are important in their number (40% of all main peak encounters) and their timing (many pre-date the first sunlit deep-dip).

According to JPL's MAVEN SPICE kernel, there will be 1959 MAVEN periapses between 2014.10.28 and 2015.10.28 (Figure 6). Of the 1798 high altitude periapses, 910, 347, 541 occur at SZAs of $<83^\circ$, 83° - 105° , and $>105^\circ$, respectively. Of the 161 deep dip periapses, 28, 73, and 60 occur at SZAs of $<83^\circ$, 83° - 105° , and $>105^\circ$, respectively. MAVEN will encounter the sunlit main peak on 101 (28+73) deep dips and 69 regular orbits (assuming 20% of the 347 regular orbits with $83^\circ < SZA < 105^\circ$). In fact, MAVEN will encounter the sunlit main peak on about 20 regular orbits (Nov. 2014) before the first deep dip campaign (Dec. 2014) and on about 15 further orbits (Feb. 2015) before the first sunlit deep dip campaign (Apr. 2015).



3 – Task A: Topside structure

Transport controls ionospheric vertical structure above ~180 km (Chen et al., 1978). The topside plasma scale height is a very sensitive indicator of the significance of vertical plasma motion. In the idealized limit that plasma transport is entirely suppressed by magnetic fields, the topside plasma scale height will be twice the neutral scale height (Schunk and Nagy, 2009) (Figure 7A). In the idealized limit that diffusive equilibrium is attained and plasma transport is unimpeded by magnetic fields, the topside plasma scale height will be $k(T_e+T_i)/m_i g$, where k is Boltzmann’s constant, T_i and T_e the ion and electron temperatures, m_i the ion mass, and g the acceleration due to gravity (Kliore, 1992) (Figure 7B). The topside plasma scale height will be on the order of 20 km in the first case and nearly an order of magnitude larger in the second case. In fact, Viking-era observations of topside plasma scale heights of tens of kilometers were used to infer the presence of horizontal magnetic fields in the ionosphere prior to the discovery of crustal magnetization by MGS (e.g., Shinagawa and Cravens, 1989, 1992; Ness et al., 2000).



In Task A, we shall characterize where and when the topside plasma scale height is controlled by the neutral atmosphere versus the plasma temperature. A simple metric suitable for use here is $X = (H_p - 2H_n)/(H_d - 2H_n)$, where H_p is the observed plasma scale height, H_n is the neutral scale height (~10 km), and H_d is $k(T_e+T_i)/m_i g$ (~150 km). X should lie between 0 and 1, near 0 if H_p is controlled by the neutral atmosphere and near 1 if controlled by the plasma temperature. We shall explore how X depends on the magnetic field, ion composition, magnetospheric conditions, and other factors, searching for patterns in when the structure of the topside ionosphere is “photochemical-like”, in diffusive equilibrium, or at different intermediate states.

In this Task, we shall use MAVEN data from NGIMS and LPW (topside plasma scale height); IUVS measurements of CO_2^+ emission (inferred topside plasma scale height); NGIMS and IUVS (neutral scale height); LPW (T_e); STATIC (T_i); and INMS and STATIC (m_i). Expected accuracies are described in the Concept Study Report (Foldout 1 and elsewhere) and the pre-AGU MAVEN Workshop presentations. Uncertainty in H_p will be a few km from LPW sweep

INTEGRATION OF MAVEN NEUTRAL AND PLASMA OBSERVATIONS

measurements of electron density with 4% accuracy every 4 seconds. Uncertainty in Hn will be ~1 km from IUVS accuracy of <3% and vertical resolution of 6 km. Uncertainty in Hd will be ~35% (based on uncertainties of 5% in LPW's Te, 25% in STATIC's Ti, and 20% in NGIMS's mi). We can also use $T_n < T_i < T_e$ to further constrain Ti if needed. Since Hd and 2Hn differ by an order of magnitude, these accuracies are sufficient to distinguish $H_p \sim 2H_n$ from $H_p \sim H_d$.

In this Task, we shall contribute to mission planning and mission operations by providing:

- Cross-calibration of different topside plasma scale height measurements;
- Cross-calibration of different neutral scale height measurements;
- Cross-calibration of different mean ion mass measurements;
- Predictions of when and where the topside ionosphere has a small (~20 km) or a large (~150 km) scale height, which affects the vertical extent of the ionosphere significantly.

4 – Task B: Topside composition

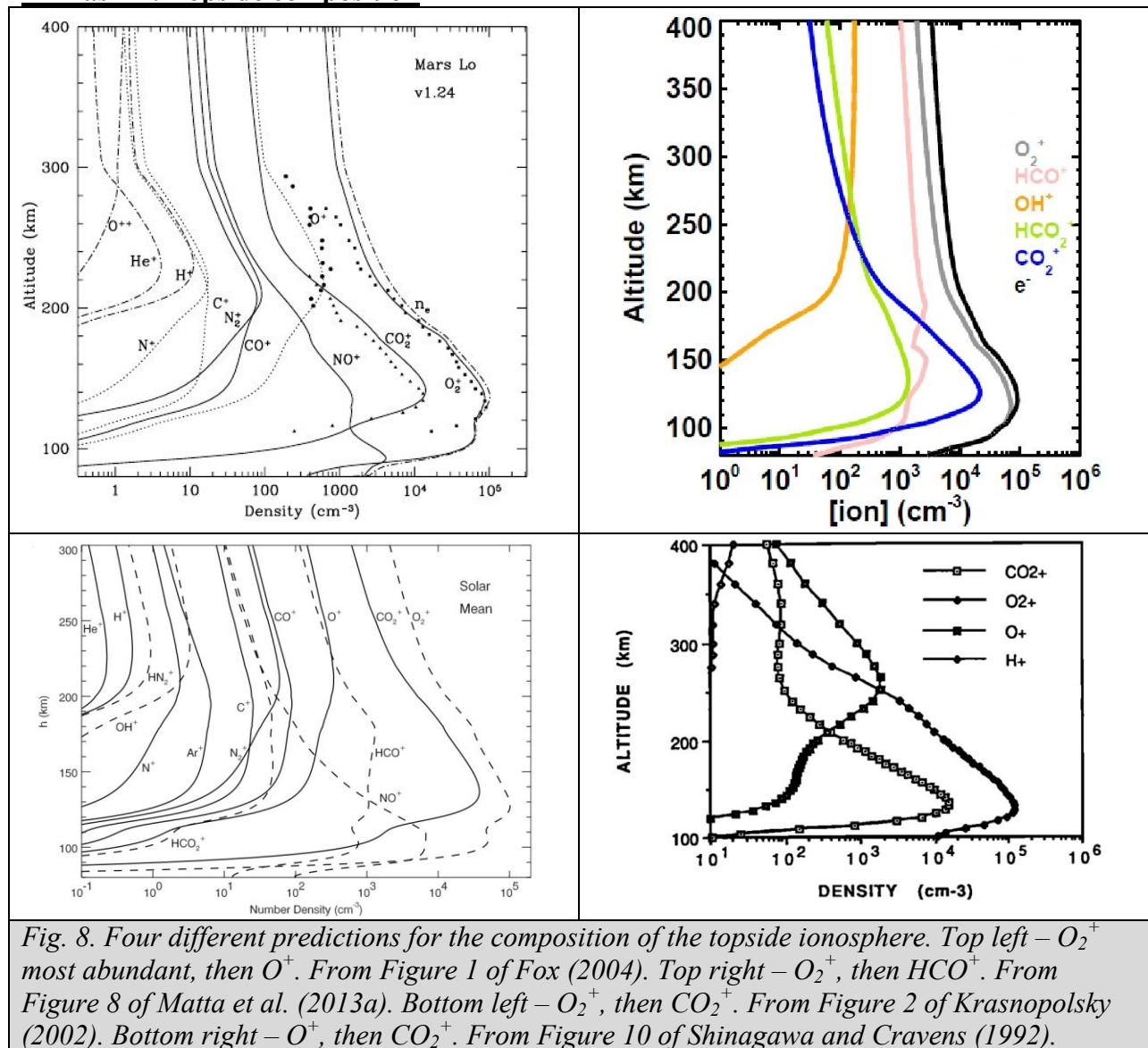


Fig. 8. Four different predictions for the composition of the topside ionosphere. Top left – O₂⁺ most abundant, then O⁺. From Figure 1 of Fox (2004). Top right – O₂⁺, then HCO⁺. From Figure 8 of Matta et al. (2013a). Bottom left – O₂⁺, then CO₂⁺. From Figure 2 of Krasnopolsky (2002). Bottom right – O⁺, then CO₂⁺. From Figure 10 of Shinagawa and Cravens (1992).

INTEGRATION OF MAVEN NEUTRAL AND PLASMA OBSERVATIONS

The composition of the topside ionosphere is important for escape. Models of the topside composition generally have O^+ , O_2^+ , and CO_2^+ as the most abundant ions, with the precise mixing ratios varying between models (Figure 8). However, a recent simulation by Matta et al. (2013a) that included more comprehensive hydrogen chemistry than usual predicted that HCO^+ may be an abundant ion above 200 km under certain circumstances (Figure 8, top right). Here the abundances of HCO^+ were greatest when H_2 abundances were high and vertical plasma transport was not suppressed by magnetic fields. Krasnopolsky (2002) also predicted the presence of substantial amounts of HCO^+ (Figure 8, bottom left).

We plan a focused investigation of the HCO^+ abundance because HCO^+ has the potential to play an important role in volatile loss at Mars, by either enhancing or impeding the loss of water. On one hand, if ionized hydrogen exists primarily as heavy HCO^+ , rather than lighter OH^+ or H^+ , then this will reduce the efficiency with which hydrogen-bearing ions are stripped away from Mars. On the other hand, when HCO^+ is neutralized by dissociative recombination into H and CO, the resultant H atom is suprathermal and highly likely to escape. The list of MAVEN Key Parameters shows that HCO^+ is not a focus of the present MAVEN team: the list does not include HCO^+ or H_2 , yet both are measureable with NGIMS 2-150 dalton range and 1 dalton resolution.

In Task B, we shall explore how the HCO^+ abundance depends on neutral composition (especially H_2 , O, CO, and CO_2) and the efficiency of vertical transport (inferred from ion velocities, the magnetic field, and the ionospheric vertical structure addressed in Task A). Once patterns are identified in the observed quantities, we shall adapt the Boston University Mars Ionospheric Model (Section 8) to attempt to reproduce them and gain insight into the processes responsible. For instance, there might be one reaction pathway that is critically important for controlling which hydrogen-bearing ion species is most abundant. We will then work with MAVEN's front-line modelers to incorporate our findings into their simulations.

In this Task, we shall use MAVEN data from NGIMS and IUVS (neutral densities); NGIMS and STATIC (ion densities); STATIC (ion velocities); MAG (field direction and strength); and LPW and NGIMS (ionospheric vertical structure). NGIMS can measure HCO^+ abundance to 20% accuracy, which is quite sufficient. If no HCO^+ is detected, we shall use the Boston University Mars Ionospheric Model to investigate why this species is absent, then focus on our other Tasks.

In this Task, we shall contribute to mission planning and mission operations by providing:

- Advocacy for the inclusion of H_2 , HCO^+ , and related species in NGIMS observing strategies and Key Parameter reports;
- Findings on whether the topside ionosphere is effectively an O^+/O_2^+ plasma and when and where its composition is more complicated;
- Model-tested hypotheses to explain observed trends in HCO^+ abundance.

5 – Task C: Electron density at the main peak

$$N_{max}^2 = [F \cos(SZA)] / [H \exp(1) 2.4E-7 \text{ cm}^3 \text{ s}^{-1} (300 \text{ K}/T_e)^{0.7}] \quad (1)$$

For idealized conditions, the peak electron density, N_{max} , satisfies equation 1 (Withers, 2009), where F is the ionizing solar flux, H is the neutral scale height, and T_e is the electron temperature. The T_e dependence appears as part of the dissociative recombination coefficient for the dominant molecular ion, O_2^+ , which equals $2.4E-7 \text{ cm}^3 \text{ s}^{-1} (300 \text{ K}/T_e)^{0.7}$. Prior work (Figure

9) shows that equation 1 is roughly satisfied at Mars (Hantsch and Bauer, 1990; Morgan et al., 2008; Withers and Mendillo, 2005; Withers, 2009), although Mars conditions are not as idealized as equation 1 suggests. Failures of equation 1 indicate areas where understanding is currently weak and discoveries possible. Equation 1 also provides a way to cross-calibrate instruments.

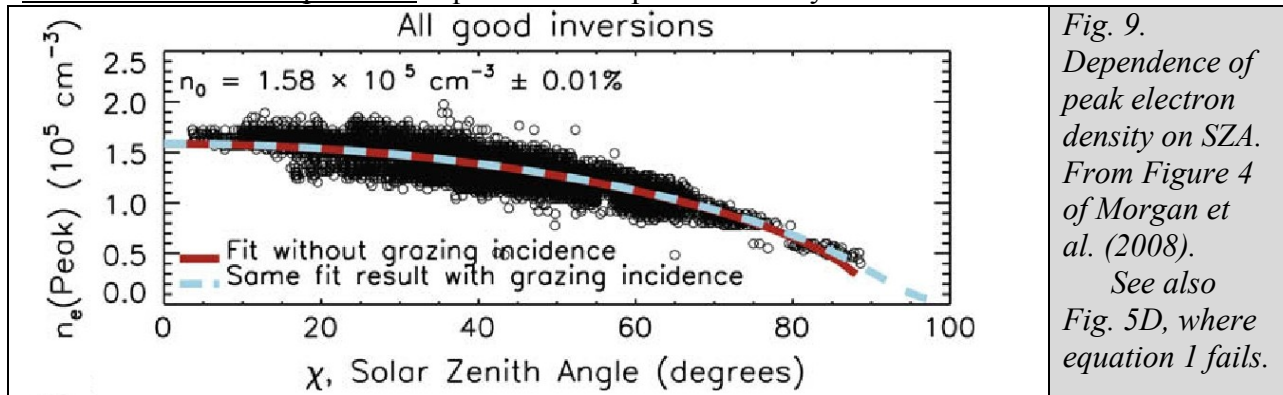


Fig. 9. Dependence of peak electron density on SZA. From Figure 4 of Morgan et al. (2008). See also Fig. 5D, where equation 1 fails.

We shall begin Task C by testing the accuracy of equation 1 using independent Nmax and H data. For instance, if equation 1 is satisfied using LPW’s Nmax, but not NGIMS’s Nmax, then the absolute calibration of NGIMS is suspect. Or, if both Nmax measurements agree, NGIMS, ACC, and IUVS H measurements agree, and F is validated against data from Earth during opposition, then equation 1 can be used to establish confidence in LPW’s measurements of Te.

We shall conclude Task C by characterizing where, when, and how equation 1 fails. We shall determine whether its failures occur in conjunction with certain atmospheric or ionospheric conditions, or unusual external forcings, which will help identify the physical processes that are responsible. For instance, equation 1 might be less accurate in strong magnetic fields (Fig. 5D), during disturbed solar conditions, or if the O/CO₂ ratio is low. Once we have identified regions/conditions where equation 1 fails (and thus exciting discoveries are possible), we will be able to predict periapses where equation 1 is likely to fail. We will work to ensure that MAVEN’s observing strategies are guided by these predictions. For many possible modes of failure, we can use and adapt an existing numerical model, the Boston University Mars Ionospheric Model (Section 8), to determine what processes are at work, then coordinate with MAVEN’s front-line modelers to incorporate our findings into their simulations. Given the model’s capabilities, this will be most fruitful for processes related to solar irradiance, or ion or neutral composition or temperature, but less fruitful for processes related to solar wind coupling.

In this Task, we shall use MAVEN data from NGIMS and LPW (Nmax); LPW/EUV/FISM (F); NGIMS, ACC, IUVS (H); LPW (Te). Constraints on Nmax are also possible from IUVS measurements of emission by CO₂⁺. Viking composition data show that the abundance of this ion is proportional to electron density (Fig. 4). If verified by MAVEN, remote CO₂⁺ emission data can be converted into electron densities. The ionizing solar flux, F, will be derived from MAVEN’s FISM model of the solar spectrum, which is driven by data from the three channels of the LPW EUV sensor (IUVS covers 110-340 nm, longward of the 90 nm ionization threshold of CO₂). We will test whether the best representation of the ionizing solar flux, F, is a simple sum of the number of ionizing photons or a sum weighted by photon energy (Lollo et al., 2012). Expected accuracies are described in the Concept Study Report (Foldout 1 and elsewhere) and the pre-AGU Community Workshop presentations. Uncertainty in Nmax from LPW sweeps will be 2%-4%. Uncertainty in H will be ~1 km from IUVS accuracy of <3% and vertical resolution

of 6 km. Uncertainty in LPW's Te will be 5%. Uncertainty in F will depend on the 10% accuracy of the LPW/EUV sensors, accuracy of extrapolation to a full FISM spectrum, and accuracy of representing F by a single number. The uncertainties in the left and right sides of equation 1 will be ~10% and ~20%, respectively, which Figs. 5D and 9 show are sufficient to test equation 1.

In this Task, we shall contribute to mission planning and mission operations by providing:

- Validation of data products from several instruments, including Te measurements that are otherwise nearly impossible to independently validate.
- Identification of regions and conditions where the ionosphere behaves unusually (i.e., equation 1 fails) and advocacy to optimize MAVEN observing strategies to target them.

6 – Task D: The neutral pressure at the main peak

The main peak is thought to occur at optical depth of unity for ionizing photons, which is equivalent to a pressure level p_m that depends on SZA as $p_m = p_0 \cos(\text{SZA})$, where p_0 is the pressure at the subsolar peak altitude (Chamberlain and Hunten, 1987). In the simplest possible representation, p_0 equals $m g / \sigma$, where m is the mean molecular mass of CO₂ (44 daltons), g is the acceleration due to gravity (3.4 m s⁻² at 150 km), and σ is the absorption cross-section of CO₂. This cross-section is of course wavelength-dependent, but a suitable characteristic value is $2\text{-}3 \times 10^{-17} \text{ cm}^2$ (Schunk and Nagy, 2009). This corresponds to $p_0 = 8\text{-}12 \times 10^{-5} \text{ Pa}$.

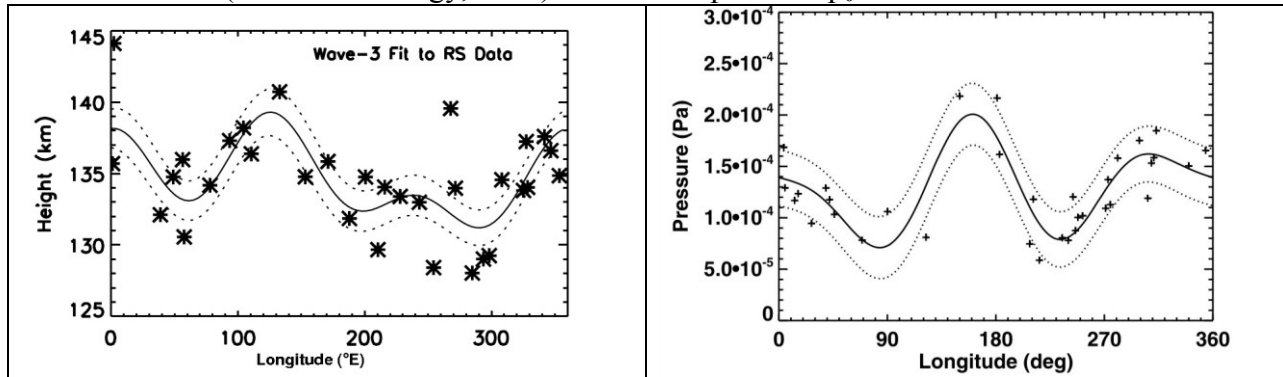


Fig. 10. The ionosphere responds as the neutral atmosphere rises and falls due to thermal tides, consistent with the peak occurring at a fixed pressure level. Left – altitude of ionospheric peak vs. longitude for selected MGS profiles at ~65°N, SZA~80°, and Ls=75°. From Figure 2 of Bougher et al. (2001). Right – neutral pressure at 110 km vs. longitude for selected SPICAM data at 40°S-30°S, Ls=150°-180°, and local time = 22-24 hrs. From Figure 2 of Withers et al. (2011).

However, there are no current simultaneous measurements of pressure and plasma density (Figure 10), so the extent to which the two predictions $p_m = p_0 \cos(\text{SZA})$ and $p_0 = 8\text{-}12 \times 10^{-5} \text{ Pa}$ are satisfied has not been established. Deviations from these expectations indicate areas where understanding is currently weak and discoveries are possible. They might occur when maximum plasma density occurs at a different altitude from maximum ionization, which might happen when electron temperatures and dissociative recombination rate coefficients change drastically with altitude, or when atypical neutral composition leads to unusual ionospheric chemistry.

In Task D, we shall see where and when the predictions $p_m = p_0 \cos(\text{SZA})$ and $p_0 = 8\text{-}12 \times 10^{-5} \text{ Pa}$ fail. For instance, deviations might be accompanied by variations in observed electron temperature or ion chemistry. We can use and adapt an existing numerical model, the Boston

INTEGRATION OF MAVEN NEUTRAL AND PLASMA OBSERVATIONS

University Mars Ionospheric Model (Section 8), to determine what processes are at work, then coordinate with MAVEN's front-line modelers to incorporate our findings into their simulations.

In this Task, we shall use MAVEN data from NGIMS and LPW (ionospheric peak altitude) and NGIMS (neutral mass densities). Neutral pressure will be found from the densities using hydrostatic equilibrium and inferred horizontal gradients. IUVS periapsis limb scans of CO_2^+ emission, which is proportional to the CO_2 density, will constrain horizontal gradients. Expected accuracies are described in the Concept Study Report (Foldout 1 and elsewhere) and the pre-AGU Community Workshop presentations. Accuracy of peak altitude will be ~ 1 km with LPW's 4 second cadence. Accuracy of pressure at the ionospheric peak will be $\sim 20\%$ due to NGIMS's 15% accuracy on neutral densities, the uncertainty in peak altitude, and effects of horizontal gradients. These are sufficient to test these predictions concerning peak pressure.

In this Task, we shall contribute to mission planning and mission operations by providing:

- Identification of regions/conditions where the ionosphere behaves unusually (i.e., pressure at ionospheric peak isn't expected value), so they can be targeted by MAVEN in subsequent orbits.
- Model-tested hypotheses to explain the observed behavior of pressure at ionospheric peak.

7 – Task E: Support for spacecraft operations inside the atmosphere

MAVEN will fly through the upper atmosphere at each periapsis. Atmospheric flight may cause heating rates to exceed allowed ranges and certain instruments to experience electrical arcing. These risks will be most pronounced during the deep dip campaigns. Consequently, neutral atmospheric conditions are of great importance for MAVEN operations. Also, MAVEN science operations begin at the same season as the Noachis storm that affected MGS operations (Keating et al., 1998; Withers and Pratt, 2013). Multiple science and engineering sensors onboard MAVEN can determine either bulk mass density or CO_2 number density, which are essentially equivalent. These include the reaction wheels (Cassini and Venus Express have derived densities from reaction wheel torques); ACC; NGIMS; IUVS (stellar occultations and periapsis limb scans of CO_2^+ emission, which is proportional to the CO_2 density); and Navigation (orbit-to-orbit changes in orbital elements will be analyzed by the engineers to provide estimates of periapsis density). It will be challenging for ACC to accurately measure densities at 150 km (Zurek, pers. comm., 2012), which is why we have not emphasized it in our preceding tasks. The 3 parts of Task E support spacecraft operations inside the atmosphere in distinct ways.

In Task E, we shall use existing software to characterize zonal variations in atmospheric conditions. Such variations were a major consideration during past aerobraking operations (e.g., Withers et al., 2003). Thermal tides generated at the surface of Mars can cause factor-of-two variations in atmospheric density with longitude at fixed altitude, season, latitude, and local time (see Figure 10 and Forbes and Hagan, 2000). We will use pre-deep-dip observations from near the deep-dip region to characterize the amplitudes/phases of the zonal variations, then report our results to the Atmospheric Advisory Group (AAG) as it plans how to lower periapsis for the deep dips. For instance, the orbit immediately before periapsis lowering might be characterized by relatively low densities and the next orbit by relatively high densities. Taken in isolation, these two points would imply a much larger scale height than is actually present, perhaps leading to a dangerous decision to descend deeper than is safe. Characterization of tidal variations will

INTEGRATION OF MAVEN NEUTRAL AND PLASMA OBSERVATIONS

prevent this. In addition, we will participate in the AAG activities that will accompany each deep-dip campaign, offering a critical perspective on accelerometer data processing, atmospheric conditions, and implications for dip strategy.

In Task E, we shall work with the IUVS team to prioritize opportunities to acquire “anchor measurements” for atmospheric densities. “Anchors” are density profiles that overlap with profiles from other instruments. MAVEN will obtain several types of in situ density profiles, plus two remotely sensed types from IUVS. These are periapsis limb scans of CO_2^+ emission and stellar occultations. The former, which are sensitive to conditions off to the side of the flight path, are proportional to CO_2 density. The latter, which provide vertical profiles of CO_2 density, will be scattered around the planet, depending on the locations of suitable stars. Comparison of these disparate datasets will be most effective if some of the remote sensing data overlap with in situ data and if some of the CO_2^+ emission profiles overlap with stellar occultation profiles.

In Task E, we shall work with MAVEN engineers to acquire time series densities determined from the reaction wheels and incorporate them into MAVEN’s PDS archive stream. Engineers on Cassini and Venus Express have produced high quality and valuable time series profiles of atmospheric densities using reaction wheels data, but these have not been archived. Since MAVEN will use PDS4 format, while our archiving experience is with PDS3, and the engineers who will generate these data products already plan to archive extensive housekeeping data, we will advocate for these densities to be added to MAVEN’s existing archive pipeline, rather than developing a separate PDS4 archiving process on our own.

In this Task, we shall contribute to mission planning and mission operations by providing:

- Characterization of zonal variations in atmospheric densities for deep-dip campaigns.
- Participation in AAG activities during deep-dip campaigns.
- Advocacy for the acquisition of IUVS “anchor measurements” for atmospheric densities.
- Efforts to archive atmospheric densities obtained from reaction wheel torques.

8 – The Boston University Mars Ionospheric Model

We will use the Boston University Mars Ionospheric Model (Fig. 11; see also Fig. 8) to identify the physical mechanisms responsible for observed features and trends. Here we briefly summarize the main characteristics of this model, which is described by Mendillo et al. (2011), Lollo et al. (2012), and Matta et al. (2013a). This proposal’s focus on the use of MAVEN data is responsible for the few words devoted to the model. The 1-D model spans 80-400 km and includes photoionization, electron-impact ionization, charge-exchange reactions, neutralization reactions, and plasma transport at a specified magnetic field inclination. Model inputs include:

- Neutral atmosphere, which is derived from the Mars Climate Database (Lewis et al., 1999);
- Solar irradiance, which is derived from the Solar2000 (Tobiska et al., 2000) or FISM (Chamberlin et al., 2007) models;
- Cross-sections and rate coefficients, taken from Schunk and Nagy (2009) and other sources;
- Representation of electron-impact ionization, based on parameterizations from other models or assuming one ionization event per ~ 34 eV of excess photon energy (Lollo et al., 2012);
- Electron and ion temperatures, which are typically based on Viking data, although the model can now solve for these self-consistently (Matta et al., 2013b, in prep.).

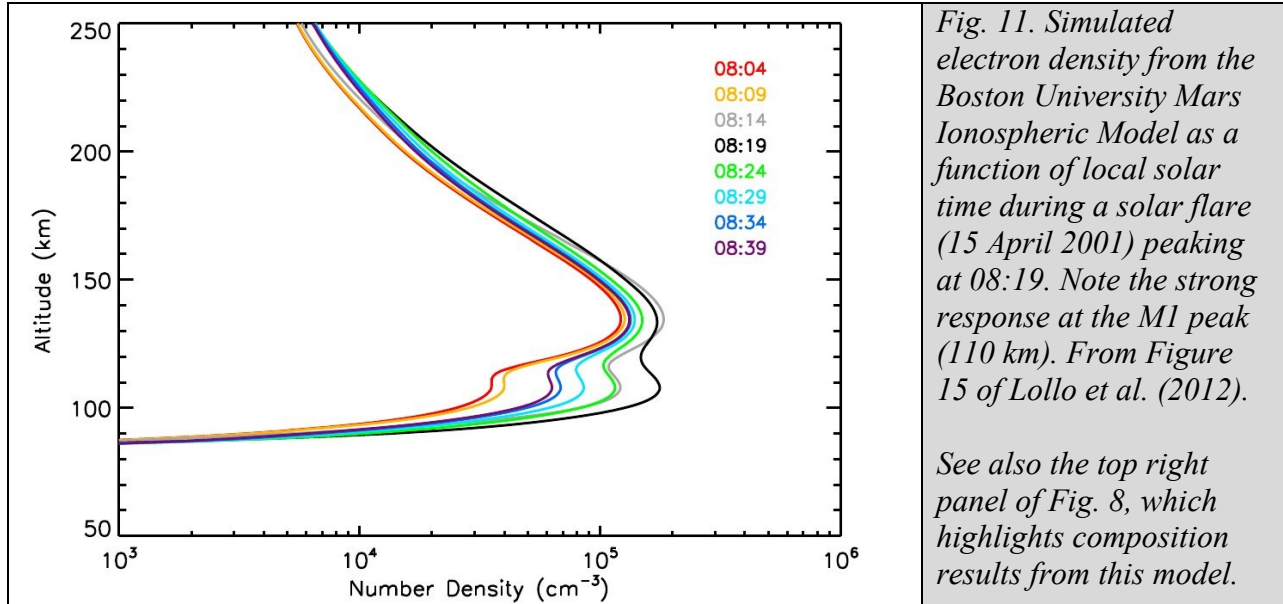


Fig. 11. Simulated electron density from the Boston University Mars Ionospheric Model as a function of local solar time during a solar flare (15 April 2001) peaking at 08:19. Note the strong response at the M1 peak (110 km). From Figure 15 of Lollo et al. (2012).

See also the top right panel of Fig. 8, which highlights composition results from this model.

We can readily run simulations in which MAVEN data specifies the neutral atmosphere (e.g., NGIMS), the solar flux (LPW/EUV/FISM), electron/ion temperatures (e.g., LPW, STATIC), and magnetic field (MAG). Upper boundary conditions on ion velocities can also be modified.

9 – Relevance to NASA and the MAVEN Participating Scientist Program

All MAVEN data needed for this proposed work, except the reaction wheel-derived densities, H₂ densities, and HCO⁺ densities, are Key Parameters (listed at the pre-AGU MAVEN Workshop).

This proposal is responsive to MAVEN Science Question #1: What is the current state of the upper atmosphere and ionosphere, and what processes control it? As such, it is directly aligned with MAVEN Participating Scientist science priority 1.3.1 – The present Mars upper atmosphere and ionosphere. Our basic strategy is to analyze MAVEN data from the upper atmosphere and ionosphere, supported by a numerical model, in order to transform better knowledge of properties (the data) into better knowledge of processes (needed for extrapolation into the past). These findings can then be used by the MAVEN front-line modelers to improve their models and better reconstruct the climate history of Mars. This approach is not currently part of the MAVEN plans. Thus our work serves as a critical link between the data the spacecraft will collect and the sophisticated models that will, as stated in the MAVEN Concept Study Report, “deliver definitive answers to long-standing questions about the climate history and habitability of Mars.”

Task E of this proposal is also aligned with MAVEN Participating Scientist science priorities 1.3.3 – Influence of the lower atmosphere on the MAVEN measurement regime – and 1.3.4 – Atmospheric waves. Thermal tides that propagate up from the lower atmosphere perturb thermospheric densities and are an important consideration for deep-dip operations. They also influence the pressure/altitude of the main ionospheric peak, which will be studied in Task D.

The proposed investigation will have an effect on and be responsive to the primary mission as it is underway. The proposed investigation cannot be accomplished by a data analysis program. This is established by the points listed at the end of the descriptions of Tasks A-E (Sections 3-7).

INTEGRATION OF MAVEN NEUTRAL AND PLASMA OBSERVATIONS

As a Co-I on the MEX radio science instrument, Withers is uniquely able to offer the MAVEN team insight into its ionospheric profiles, which are currently only accessible to instrument team members. Even experimenters on other MEX instruments do not have access. We are not able to disseminate MEX data, but we can share images of all profiles and details of profile locations or dates. Given the limited access granted so far to MEX personnel outside the radio science team, it is extremely unlikely that any project-level MAVEN-MEX Memorandum of Understanding will lead to the MAVEN team receiving digital copies of all MEX radio occultation profiles.

10 – Personnel and Work Plan

This investigation will be conducted by PI Paul Withers (Boston University, BU), a BU postdoc, and collaborator Scott Guzewich (JHU). We budget 3.6m funded effort for Withers and 18.25m funded effort for the postdoc. Withers's effort is budgeted as release from half of his teaching commitments in Fall 2014 (start of science mission) and again in Fall 2015 (end of science mission), which permits flexibility in focusing his efforts into the 365 day prime science mission.

Paul Withers, Professor in the Astronomy Department of Boston University, will be responsible for the success of this investigation and for compliance with all reporting requirements. He is well-placed to lead an investigation into the integration of MAVEN neutral and plasma observations. He has completed a range of studies on the ionosphere of Mars, including the effects of solar energetic particle events, meteoroid influx, crustal fields (both observational and theoretical), solar flares, and other solar variations (Withers and Mendillo, 2005; Withers et al., 2005, 2008, 2012a, 2012b; Withers, 2008, 2009, 2011; Mendillo et al., 2006, 2011; Opgenoorth et al., 2010; Lillis et al., 2010; Lollo et al., 2012). He has also worked extensively on the neutral atmosphere of Mars (Withers et al., 2003, 2011; Withers, 2012a; Withers and Smith, 2006; Withers and Catling, 2010; Withers and Pratt, 2013; Bougher et al., 2006; Vasavada et al., 2013). Withers participated in AAGs for the landings of Spirit, Opportunity, and Curiosity; was responsible for atmospheric reconstruction for the landings of these three missions and Phoenix; supported aerobraking operations for MGS and Mars Odyssey; is/was a Co-Investigator on numerous spacecraft instruments, including VEX and MEX radio science, Huygens HASI, ExoMars Entry Science, and Mars Odyssey accelerometer; and provided MAVEN Critical Data Products concerning neutral upper atmospheric variability (relevant to Tasks D and E).

A Boston University postdoctoral researcher will be hired to perform the bulk of the proposed work. Due to extensive recent hiring of our potential postdocs at MAVEN lead institutions Berkeley and Colorado, we have not yet recruited an individual to fill this position. Current graduate student Majd Matta (BU) is a possibility, as well as graduating students from Michigan, Berkeley, and other institutions. If necessary, we shall use graduate students or staff researchers as a stopgap measure until a suitable postdoc is hired.

Collaborator Scott Guzewich (JHU graduate student, soon to be GSFC postdoc) works on the dynamics of the Mars atmosphere, particularly thermal tides in the middle atmosphere (Guzewich et al., 2010, 2011, 2012a, b, c). This complements Withers's familiarity with tides in the upper atmosphere. Guzewich will support the neutral upper atmospheric studies of Tasks D and E by providing a middle atmosphere context derived from his work on existing projects.

INTEGRATION OF MAVEN NEUTRAL AND PLASMA OBSERVATIONS

This proposal involves data from multiple MAVEN instruments, so we do not expect to be sufficiently tied to a particular instrument to justify visiting that instrument lead's facility regularly. Quarterly MAVEN science team meetings and innumerable telecons provide ample opportunities for collaborations. As is clear from the outlines of our tasks, our main interactions will be with the NGIMS, LPW, and IUVS teams. It will be straight-forward for us to meet with these teams, if necessary, since NGIMS is led from Goddard, which can be visited on an inexpensive daytrip from Boston, LPW is led from Colorado, where many MAVEN project-level meetings will be held, and IUVS is represented at BU by MAVEN Co-I John Clarke.

We are excited to participate in the MAVEN EPO efforts. In addition to providing science nuggets to the project-level EPO effort, we will coordinate with the EPO leads to write annual Eos articles summarizing the overall discoveries of the mission (Withers, 2005, 2012b).

Nominally, roughly equal effort will be devoted to Tasks A-E. The large number of tasks may appear to be a weakness. However, it actually provides resilience. Spacecraft and instrument performance issues (good and bad) and unexpected scientific discoveries may make it impractical to start a task until a glitch is fixed, render a task impossible, or show that a task is not as rewarding as expected. If so, we can simply focus on the remaining tasks. Also, the data analysis aspects of Tasks A-D are relatively straight-forward.

Year 1 (Approximately launch to end of on-orbit commissioning, 12 months)

Write Implementation Plan; Develop software to manipulate MAVEN Key Parameter data in support of proposed tasks; Prepare model to run with MAVEN-specified inputs; Collaborate with instrument teams to develop deeper understanding of planned instrument performance, operational modes, and observing sequences; Contribute to operational planning.

Postdoctoral researcher (7.5 months) responsible for progress, with support from Withers.

Deliverables: Implementation Plan (month 0); Report on status of software development (quarterly); Contributions to operational planning (quarterly); Semi-annual reports.

Year 2 (Approximately primary science mission, 12 months)

Contribute to mission operations as outlined in tasks; Start and make substantial progress on Tasks A-D; Complete Task E; Contribute to "first results" manuscripts led by senior MAVEN personnel (e.g., instrument leads, science theme leads); Develop outlines of four manuscripts summarizing Tasks A-D; submit first Eos article.

Postdoctoral researcher (7.5 months) primarily responsible for scientific progress on Tasks A-D, jointly responsible for progress on manuscripts; Withers (1.8 months, 50% buyout of Fall 2014 teaching commitment) primarily responsible for operational contributions and Task E, jointly responsible for progress on manuscripts; Collaborator Guzewich will support Tasks D-E.

Deliverables: Support for deep-dip campaigns (approximately every 2 months); Other support for mission operations (recurring); Eos manuscript (month 18); Semi-annual reports.

Year 3 (Approximately post-primary mission data analysis, 6 months)

Re-visit results of Tasks A-D with post-primary mission perspective; Complete drafts of four manuscripts summarizing Tasks A-D; submit second Eos article.

Postdoctoral researcher (3.25 months) primarily responsible for post-primary mission perspective and for two manuscripts; Withers primarily responsible for two manuscripts.

Deliverables: 4 scientific articles (month 30); Eos manuscript (month 30); Semi-annual reports.

References

Angelats i Coll et al. (2004) Upper atmosphere of Mars up to 120 km: Mars Global Surveyor data analysis with the LMD general circulation model, *J. Geophys. Res.* 109, E01011, doi:10.1029/2003JE002163.

Angelats i Coll et al. (2005) The first Mars thermospheric general circulation model: The Martian atmosphere from the ground to 240 km, *Geophys. Res. Lett.* 32, L04201, doi:10.1029/2004GL021368.

Barth et al. (1992) Aeronomy of the current martian atmosphere, in Mars, eds. Kieffer, H., Jakosky, B., Snyder, C., and Matthews, M., pp. 1054-1089, University of Arizona Press.

Bell et al. (2007) Vertical dust mixing and the interannual variations in the Mars thermosphere, *J. Geophys. Res.* 112, E12002, doi:10.1029/2006JE002856.

Bougher et al. (2001) Mars Global Surveyor Radio Science electron density profiles: Neutral atmosphere implications, *Geophys. Res. Lett.* 28, 3091-3094, doi:10.1029/2001GL012884.

Bougher et al. (2002) Simulations of the upper atmospheres of the terrestrial planets. In *Atmospheres in the Solar System, Comparative Aeronomy* (ed. M. Mendillo, A. F. Nagy and J. H. Waite, Jr.), AGU Monograph #130, Washington, D.C.: American Geophysical Union, pp. 261-288.

Bougher et al. (2006) Polar warming in the Mars thermosphere: Seasonal variations owing to changing insolation and dust distributions, *Geophys. Res. Lett.* 33, L02203, doi:10.1029/2005GL024059.

Bougher et al. (2008) Neutral upper atmosphere and ionosphere modeling, *Space Sci. Rev.* 139, 107-141, doi:10.1007/s11214-008-9401-9.

Bougher et al. (2013) Upper neutral atmosphere and ionosphere, in *The atmosphere of Mars* (eds. Haberle et al.), Cambridge University Press.

Brain et al. (2010) A comparison of global models for the solar wind interaction with Mars, *Icarus*, 206, 139-151

Brecht and Ledvina et al. (2006) The solar wind interaction with the Martian ionosphere/atmosphere, *Space Sci. Rev.* 126, 15–38.

Chamberlain and Hunten (1987) *Theory of planetary atmospheres*, Academic Press.

Chamberlin et al. (2007) Flare Irradiance Spectral Model (FISM): Daily component algorithms and results, *Space Weather*, 5, S07005, doi:10.1029/2007SW000316.

INTEGRATION OF MAVEN NEUTRAL AND PLASMA OBSERVATIONS

Chen et al. (1978) The martian ionosphere in light of the Viking observations, *J. Geophys. Res.*, 83, 3871-3876.

Fang et al. (2010a) Escape probability of Martian atmospheric ions: Controlling effects of the electromagnetic fields, *J. Geophys. Res.*, 115, A04308, doi:10.1029/2009JA014929

Fang et al. (2010b) On the effect of the martian crustal magnetic field on atmospheric erosion, *Icarus*, 206, 130-138.

Forbes and Hagan (2000) Diurnal Kelvin wave in the atmosphere of Mars: Towards an understanding of “stationary” density structures observed by the MGS Accelerometer, *Geophys. Res. Lett.* 27, 21, doi:10.1029/2000GL011850.

Forget et al. (1999) Improved general circulation models of the Martian atmosphere from the surface to above 80 km, *J. Geophys. Res.* 104, 24,155–24,175.

Fox et al. (1996) The thermosphere/ionosphere of Mars at high and low solar activities, *Adv. Space Res.* 17, 203-218.

Fox (2004) Response of the Martian thermosphere/ionosphere to enhanced fluxes of solar soft X rays, *J. Geophys. Res.* 109, A11310, doi:10.1029/2004JA010380.

Fox and Yeager (2006) Morphology of the near-terminator Martian ionosphere: a comparison of models and data, *J. Geophys. Res.* 111, A10309, doi:10.1029/2006JA011697.

Fox (2009) Morphology of the dayside ionosphere of Mars: Implication for ion outflows, *J. Geophys. Res.* 114, E12005, doi:10.1029/2009JE003432.

González-Galindo et al. (2005) Extension of a Martian general circulation model to thermospheric altitudes: UV heating and photochemical models, *J. Geophys. Res.* 110, E09008, doi:10.1029/2004JE002312.

González-Galindo et al. (2009a) A ground-to-exosphere Martian general circulation model: 1. Seasonal, diurnal, and solar cycle variation of thermospheric temperatures, *J. Geophys. Res.* 114, E04001, doi:10.1029/2008JE003246.

González-Galindo et al. (2009b) A ground-to-exosphere Martian general circulation model: 2. Atmosphere during solstice conditions—Thermospheric polar warming, *J. Geophys. Res.* 114, E08004, doi:10.1029/2008JE003277.

González-Galindo et al. (2010) Thermal and wind structure of the Martian thermosphere as given by two general circulation models, *Planet. Space Sci.* 58, 1832-1849, doi:10.1016/j.pss.2010.08.013.

Guzewich et al. (2010) Observations of planetary and tidal waves as seen by the Mars Climate Sounder, Fall AGU Meeting, abstract #P53E-1554.

INTEGRATION OF MAVEN NEUTRAL AND PLASMA OBSERVATIONS

Guzewich et al. (2011) Analysis of tides in a MarsWRF simulation forced with TES limb dust observations, Fall AGU Meeting, abstract #P21A-1637.

Guzewich et al. (2012a) Observations of planetary waves and nonmigrating tides by the Mars Climate Sounder, *J. Geophys. Res.*, 117, E03010, doi:10.1029/2011JE003924

Guzewich et al. (2012b) Measurement of Mars atmospheric winds with interferometry, Workshop on Concepts and Approaches for Mars Exploration, held June 12–14, 2012 in Houston, Texas. LPI Contribution No. 1679, id.4138

Guzewich et al. (2012c) Inter-annual variability of high-altitude dust layers on Mars and their connection with the general circulation, Workshop on Comparative Climatology of Terrestrial Planets, held June 25–28, 2012, in Boulder, Colorado. LPI Contribution No. 1675, id.8025

Hanson et al. (1977) The Martian ionosphere as observed by the Viking retarding potential analyzers, *J. Geophys. Res.* 82, 4351–4363.

Hanson and Mantas (1988) Viking electron temperature measurements — Evidence for a magnetic field in the Martian ionosphere, *J. Geophys. Res.* 93, 7538–7544.

Hantsch and Bauer (1990) Solar control of the Mars ionosphere, *Planet. Space Sci.*, 38, 539-542

Kliore (1992) Radio occultation observations of the ionospheres of Mars and Venus, in *Venus and Mars: Atmospheres, ionospheres, and solar wind interactions*, eds. Luhmann, J., Tatrallyay, and Pepin, R., pp. 265-276, AGU Press.

Krasnopolsky (2002) Mars' upper atmosphere and ionosphere at low, medium, and high solar activities: Implications for evolution of water, *J. Geophys. Res.* 107, 5128–5139.

Leblanc and Johnson (2002) Role of molecular species in pickup ion sputtering of the Martian atmosphere, *J. Geophys. Res.*, 107, 5010, doi:10.1029/2000JE001473.

Lewis et al. (1999) A climate database for Mars, *J. Geophys. Res.* 104, 24177–24194.

Liemohn et al. (2006) Mars global MHD predictions of magnetic connectivity between the dayside ionosphere and the magnetospheric flanks, *Space Sci. Rev.*, 126, 63-76.

Lillis et al. (2010) Total electron content in the Mars ionosphere: Temporal studies and dependence on solar EUV flux, *Geophys. Res. Lett.*, 115, A11314, doi:10.1029/2010JA015698.

Lollo et al. (2012) Numerical simulations of the ionosphere of Mars during a solar flare, *J. Geophys. Res.*, 117, A05314, doi:10.1029/2011JA017399.

Ma et al. (2004) Three-dimensional, multispecies, high spatial resolution MHD studies of the solar wind interaction with Mars, *J. Geophys. Res.*, 109, A07211, doi:10.1029/2003JA010367.

INTEGRATION OF MAVEN NEUTRAL AND PLASMA OBSERVATIONS

- Ma and Nagy (2007) Ion escape fluxes from Mars, *Geophys. Res. Lett.* 34, L08201, 10.1029/2006GL029208, 2007.
- Matta et al. (2013a) The composition of Mars' topside ionosphere: Effects of hydrogen, *J. Geophys. Res.*, doi:10.1002/jgra.50104, in press.
- Matta et al. (2013b) Simulated electron and ion temperatures in the ionosphere of Mars: Diurnal cycle, in preparation for submission to *J. Geophys. Res.*
- Mendillo et al. (2006) Effects of solar flares on the ionosphere of Mars, *Science*, 311, 1135-1138.
- Mendillo et al. (2011) Modeling Mars' ionosphere with constraints from same-day observations by Mars Global Surveyor and Mars Express, *J. Geophys. Res.*, 116, A11303, doi:10.1029/2011JA016865.
- McDunn et al. (2010) Simulating the density and thermal structure of the middle atmosphere (80-130 km) of Mars using the MGCM-MTGCM: A comparison with MEX/SPICAM observations, *Icarus* 206, 5–17.
- Modolo et al. (2006) Simulated solar wind plasma interaction with the martian exosphere: Influence of the solar EUV flux on the bow shock and the magnetic pile-up boundary, *Ann. Geophys.*, 24, 3403-3410.
- Moffat-Griffin et al. (2007) Thermal structure and dynamics of the Martian upper atmosphere at solar minimum from global circulation model simulations, *Ann. Geophys.* 25, 2147-2158.
- Morgan et al. (2008) Variation of the martian ionospheric electron density from Mars Express radar soundings, *J. Geophys. Res.*, 113, A09303, doi:10.1029/2008JA013313
- Ness et al. (2000) Effects of magnetic anomalies discovered at Mars on the structure of the martian ionosphere and solar wind interaction as follows from radio occultation experiments, *J. Geophys. Res.*, 105, 15,991-16,004.
- Nielsen et al. (2007) Local plasma processes and enhanced electron densities in the lower ionosphere in magnetic cusp regions on Mars, *Planet. Space Sci.* 55, 2164–2172.
- Nier and McElroy (1977) Composition and structure of Mars' upper atmosphere: Results from the Neutral Mass Spectrometers on Viking 1 and 2, *J. Geophys. Res.* 82, 4341–4349.
- Opgenoorth et al. (2010) Dayside ionospheric conductivities at Mars, *Planet. Space Sci.*, 58, 1139-1151.
- Schunk and Nagy (2009) *Ionospheres*, Cambridge University Press.

INTEGRATION OF MAVEN NEUTRAL AND PLASMA OBSERVATIONS

- Seiff and Kirk (1977) Structure of the atmosphere of Mars in summer at mid-latitudes, *J. Geophysical Res.* 82, 4364–4378.
- Shinagawa and Cravens (1989) A one-dimensional multispecies magnetohydrodynamic model of the dayside ionosphere of Mars, *J. Geophys. Res.* 94, 6506–6516.
- Shinagawa and Cravens (1992) The ionospheric effects of a weak intrinsic magnetic field at Mars, *J. Geophys. Res.*, 97, 1027-1035.
- Stewart et al. (1972) Mariner 9 ultraviolet spectrometer experiment: Structure of Mars's upper atmosphere, *Icarus* 17, 469–474.
- Tobiska et al. (2000) The SOLAR2000 empirical solar irradiance model and forecast tool, *J. Atmos. Solar-Terr. Physics*, 62, 1233-1250.
- Vaille et al. (2009a) Three-dimensional study of Mars upper thermosphere/ionosphere and hot oxygen corona: 1. General description and results at equinox for solar low conditions, *J. Geophys. Res.*, 114, E11005, doi:10.1029/2009JE003388.
- Vaille et al. (2009b) Three-dimensional study of Mars upper thermosphere/ionosphere and hot oxygen corona: 2. Solar cycle, seasonal variations, and evolution over history, *J. Geophys. Res.*, 114, E11006, doi:10.1029/2009JE003389.
- Vaille et al. (2010) A study of suprathermal oxygen atoms in Mars upper thermosphere and exosphere over the range of limiting conditions, *Icarus*, 206, 18-27.
- Vasavada et al (2012) Assessment of environments for Mars Science Laboratory entry, descent, and surface operations, *Space Sci. Rev.*, 170, 793-835
- Withers (2005) What is a planet? *Eos*, 86, 326, doi:10.1029/2005EO360004.
- Withers et al. (2003) The effects of topographically-controlled thermal tides in the martian upper atmosphere as seen by the MGS accelerometer, *Icarus*, 164, 14-32
- Withers and Mendillo (2005) Response of peak electron densities in the martian ionosphere to day-to-day changes in solar flux due to solar rotation, *Planet. Space Sci.*, 53, 1401-1418, doi:10.1016/j.pss.2005.07.010
- Withers et al. (2005) Ionospheric characteristics above martian crustal magnetic anomalies, *Geophys. Res. Lett.*, 32, L16204, doi:10.1029/2005GL023483.
- Withers (2006) Mars Global Surveyor and Mars Odyssey accelerometer observations of the Martian upper atmosphere during aerobraking, *Geophys. Res. Lett.* 33, L02201, doi:10.1029/2005GL024447.

INTEGRATION OF MAVEN NEUTRAL AND PLASMA OBSERVATIONS

Withers and Smith (2006) Atmospheric entry profiles from the Mars Exploration Rovers Spirit and Opportunity, *Icarus*, 185, 133-142, doi:10.1016/j.icarus.2006.06.013.

Withers (2008) Theoretical models of ionospheric electrodynamics and plasma transport, *J. Geophys. Res.*, 113, A07301, doi:10.1029/2007JA012918.

Withers et al. (2008) Physical characteristics and occurrence rates of meteoric plasma layers detected in the Martian ionosphere by the Mars Global Surveyor Radio Science Experiment, *J. Geophys. Res.*, 113, A12314, doi:10.1029/2008JA013636.

Withers (2009) A review of observed variability in the dayside ionosphere of Mars, *Adv. Space Res.*, 44, 277-307.

Withers and Catling (2010) Observations of atmospheric tides at the season and latitude of the Phoenix atmospheric entry, *Geophys. Res. Lett.*, 37, L24204, doi:10.1029/2010GL045382.

Withers (2011) Attenuation of radio signals by the ionosphere of Mars: Theoretical development and application to MARSIS observations, *Radio Science*, 46, doi:10.1029/2010RS004450.

Withers et al. (2011) Observations of thermal tides in the middle atmosphere of Mars by the SPICAM instrument, *J. Geophys. Res.*, 116, E11005, doi:10.1029/2011JE003847.

Withers (2012a) Empirical predictions of martian surface pressure in support of the landing of Mars Science Laboratory, *Space Sci. Rev.*, 170, 837-860.

Withers (2012b) How do meteoroids affect Venus's and Mars's ionospheres? *Eos*, 93, 337-338, doi:10.1029/2012EO350002.

Withers et al. (2012a) A clear view of the multifaceted dayside ionosphere of Mars, *Geophys. Res. Lett.*, 39, L18202, doi:10.1029/2012GL053193.

Withers et al. (2012b) Observations of the nightside ionosphere of Mars by the Mars Express Radio Science Experiment (MaRS), *J. Geophys. Res.*, 117, A12307, doi:10.1029/2012JA018185.

Withers and Pratt (2013) An observational study of the response of the upper atmosphere of Mars to lower atmospheric dust storms, *Icarus*, in press.